Electronic Supplementary Information (ESI)

BODIPYs revealing lipid droplets as valuable targets for photodynamic theragnosis

Andrea Tabero,[a] Fernando García-Garrido,[b] Alejandro Prieto-Castañeda,[b] Eduardo Palao,[b] Antonia R. Agarrabeitia,[b] Inmaculada García-Moreno,[c] Angeles Villanueva,[a,d] Santiago de la Moya,[b,*] and María J. Ortiz[b,*]

[a] Departamento de Biología, Universidad Autónoma de Madrid, Darwin 2, 28049 Madrid, Spain.
[b] Departamento de Química Orgánica, Facultad de CC. Químicas, Universidad Complutense de Madrid, Ciudad Universitaria s/n, 28040 Madrid, Spain.
E-mail: mjortiz@quim.ucm.es, santmoya@ucm.es
[c] Departamento de Sistemas de Baja Dimensionalidad, Superficies y Materia Condensada, Instituto de Química-Física Rocasolano, Centro Superior de Investigaciones Científicas (CSIC), Serrano 119, 28006 Madrid, Spain.
[d] Instituto Madrileño de Estudios Avanzados (IMDEA) Nanociencia, Ciudad Universitaria de Cantoblanco, 28049 Madrid, Spain.

Table of contents

1. General methods

1.1. Synthesis

All starting materials and reagents were commercial, unless otherwise indicated, and used without further purifications. Common solvents were dried and distilled by standard procedures. Flash chromatography was performed using silica gel (230-400 mesh). NMR spectra were recorded using $CDCl_3$ at 20 ºC. ^{1}H NMR and ^{13}C NMR chemical shifts (δ) were referenced to internal solvent $CDCl_3$ (δ = 7.260 and 77.03 ppm, respectively). DEPT 135 experiments were used to determine the type of carbon nucleus (C *vs.* CH *vs.* CH_2 *vs.* CH_3). FTIR spectra were obtained from neat samples using the ATR technique. High resolution mass spectrometry (HRMS) were performed using the EI technique.

1.2. Fundamental optical properties

Photophysical properties were registered in diluted solutions (*ca.* $1x10^{-5}$ M), prepared by diluting a concentrated stock solution in ethyl acetate. UV-Vis absorption and fluorescence spectra were recorded on a Bio-Tek spectrophotometer (model UVIKON XL) and a Sim-Aminco spectrofluorimeter (model Aminco Bowman Series 2), respectively. The fluorescence spectra were corrected from the wavelength dependence of de detector sensitivity. Commercial PM546 (1,3,5,7,8-penta-methylBODIPY) was used as the reference dye (ϕ = 0.85 in ethyl acetate)[1].

1.3. Photostability

Photostability was evaluated by pumping transversely 10 μL of a dye solution in ethyl acetate (10^{-3} M) at 355 nm, with 4-mJ 8-ns FWHM pulses from the third-harmonic of a Q-switched Nd:YAG laser (Spectron SL282G), at a repetition rate of up to 10 Hz. The solutions were contained in a cylindrical Pyrex tube (1-cm height, 1-mm internal diameter) carefully sealed to avoid solvent evaporation during the experiments. The laser exciting pulses were line-focused onto the tube, providing pump fluences on the active medium in the range 110-180 mJ/cm^2. The fluorescence emission was monitored perpendicular to the exciting beam, collected by an optical fiber, imaged onto the input slit of a monochromator (Acton Research corporation) and detected with a charge-coupled device (CCD) (SpectruMM:GS128B). Each experience was

repeated at least three times. The estimated error in the energy and photostability measurements is 10%.

1.4. Cell cultures

HeLa (ATCC® CCL-2™) and Hs68 (ATCC® CRL-1635™) cells were grown as monolayer cultures in Dulbecco's Modified Eagle's Medium (DMEM) supplemented with 10% (v/v) fetal bovine serum (FBS), 50 $U \cdot mL^{-1}$ penicillin and 50 $\mu g \cdot mL^{-1}$ streptomycin. All products were purchased from Thermo Fisher Scientific (Waltham, MA, USA) and sterilized by means of 0.22 µm filters (Merck Millipore, Billerica, MA, USA). Cell cultures were performed in a 5% CO_2 atmosphere plus 95% air at 37 °C, and maintained in a SteriCult 200 (Hucoa-Erloss, Madrid, Spain) incubator. Subconfluent cell cultures seeded in 24-well plates (with or without coverslip, depending on the experiment) were used to perform the experiments. All sterile plastics were purchased from Corning (New York, NY, USA).

1.5. Evaluation of the PDT activity

After incubation with the corresponding dye (1-10 µM) during 24 h, cells were washed 3 times with culture medium and irradiated with 10.3 J/cm^2 of green light (518 ± 10 nm). After irradiation, cells were maintained protected from light in the incubator for 24 h. Then, cell viability was evaluated by MTT [3-(4,5-dimethylthiazol-2-yl)-2,5-diphenyltetrazolium bromide] assay.

For conducting the MTT assay, cells were incubated with 50 $\mu g \cdot mL^{-1}$ solution of MTT (Sigma Aldrich) in culture medium (from an initial MTT stock of 1 $mg \cdot mL^{-1}$ in PBS) for 3 h. Then, generated formazan was extracted with 500 µL dimethyl sulfoxide (DMSO), and absorbance was measured at 542 nm in a SpectraFluor spectrophotometer (Tecan Group Ltd, Männedorf, Switzerland). Cell survival was expressed as the percentage of absorption of treated cells in comparison with that of control cells. Statistical significance for surviving-fraction data acquired from the conducted MTT assays is obtained by using one-way ANOVA (all groups *vs.* control group) Statistically significant differences are labelled as * ($p < 0.001$). DMSO in dyes solutions (up to 0.2% in the 10 µM solution) was checked to have no influence on cell viability (data not shown).

1.6. Localization experiments

Two experimental incubation conditions were selected to analyze the subcellular localization of the studied BODIPY dyes by fluorescence microscopy: (1) incubation with 5 μM dye for 24 h; (2) incubation with 75 nM dye for 1 h. Dye solution in culture medium was prepared from an initial 5 mM dye stock-solution in DMSO (Panreac, Barcelona, Spain). After incubating with the corresponding dye, cells were washed three times with PBS and observed by confocal or epifluorescence microscopy.

To promote massive LD accumulation into the cells, cells were incubated with fresh sunflower-oil emulsion prior to their incubation with the corresponding dye. The said oil emulsion was prepared as reported by Stockert *et al.*[2]. Thus, commercial sunflower oil and DMEM were mixed in 1:1 v/v ratio and filtered through 0.45 μm filter (Merck Millipore, Billerica, MA, USA). The obtained oil emulsion was mixed with the culture medium in 1:6 v/v ratio, and incubated for 18 h prior to the incubation with the corresponding dye.

To localize lysosomes in HeLa cells, acidic compartments of HeLa cells were labeled with LysoTracker® Red DND-99 (50 nM, ThermoFisher, USA) in the culture medium at 37 °C for 30 min. After labeling, cells were washed with PBS and observed by fluorescence microscopy.

To localize mitochondria in HeLa cells, these organelles were labeled with MitoTracker® Green (200 nM, ThermoFisher, USA) in the culture medium at 37 °C for 30 min. After labeling, cells were washed with PBS and observed by fluorescence microscopy.

To localize lipid droplets (LDs) in HeLa cell, lipids were stained with Oil Red O (ORO).[3] For this purpose, the Lipir (Oil Red O) Staining Kit (K580-24, BioVision, San Francisco, CA, USA) was used following the kit instructions. The cells were observed by under-bright-field microscopy and fluorescence microscopy.

1.7. Detection of ROS participation

Intracellular ROS levels after photodynamic treatments were determined using 2´,7´-dichlorodihydrofluorescein diacetate (DCFH-DA) as fluorogenic probe.[4] Thus, 1 h after incubation with the corresponding dye, or after incubation and subsequent irradiation, cells were incubated with DCFH-DA 5 μM for 30 min, washed and observed by fluorescence microscopy.

Participation of $^1O_2$ in the PDT acticivity was determined by quenching such ROS with sodium azide (NaN_3).[5] For this purposse, NaN_3 (5 mM) was added to the cell-culture 2 h prior to irradiation (PDT treatment), and the cytotoxicity evaluated by MTT assay 24 h after treatment and compared with paralell experiment without addind the quenceher.

1.8. Characterization of cell-death mechanisms

Apoptosis was identified by morphological criteria under light microscopy (phase contrast or differential interference contrast, DIC),[6] as well as by indirect immunofluorescence detection of Cytochrome c or Caspase-3 activated proteins.[7] For this purpose, HeLa cells on coverslips were fixed in 4% PFA for 20 min at 4 °C, washed three times with PBS (5 min each), and permeabilized with 0.5% Triton X-100. After 5 min, Triton X-100 was removed and cells were incubated in blocking solution (5% bovine serum albumin, 5% FBS, 0.02% Triton X-100 in PBS) for 30 min at RT. Once removed from blocking solution, 25 µl of a 1:50 solution of primary antibody (monoclonal mouse anti-cytochrome c; Santa Cruz Biotechnology, Santa Cruz, CA, USA) was added to each sample and incubated at 37 °C for 1 h. Three 5-min washings with PBS were then carried out before addition of Triton X-100 for 5 min. Incubation of secondary antibody (1:100 Fab specific goat anti-mouse IgG Alexa Fluor 488; Thermo Fisher Scientific) was identical to that of the first one and so were final washings. Cells were counterstained using Hoechst-33258 and mounted with ProLong Gold antifade reagent. For detection of active caspase-3, a similar protocol was used to that described for cytochrome c. A solution 1:100 of primary monoclonal rabbit anti-cleaved caspase-3 antibody (9664S, Cell Signaling Technology; Danvers, MA, USA) and 1:300 a solution of secondary antibody goat anti-rabbit IgG bounded to Alexa Fluor® 555 (A21428, Thermo Fisher Scientific) were used.

1.9. Multicolour imaging

Multicolour experiment involving the detection of LDs, microtubules and DNA: After incubating HeLa cells with the corresponding dye (75 nM for 1 h), the cells on coverslips were fixed in 4% PFA for 20 min at 4 °C, washed three times with PBS, and permeabilized with 0.5% Triton X-100. After 5 min, Triton X-100 was removed, and the cells incubated in blocking solution (5% bovine serum albumin, 5% FBS,

0.02% Triton X-100 in PBS) for 15 min at R.T. Once removed the blocking solution, 1:100 v/v solution of α-tubulin antibody (monoclonal mouse anti-α-tubulin antibody; Sigma Aldrich, St. Louis, MO, USA) was added to the cells and incubated at 37 °C for 1 h. Three 5-min washings with PBS were then carried out before addition of Triton X-100 for 5 min. Incubation with the secondary antibody (1:100 v/v Alexa Fluor 488 goat anti-mouse IgG; Invitrogen) and subsequent washings were identically conducted to those performed with the first antibody. Finally, the cells were counterstained using H-33258 (Hoechst-33258; Sigma-Aldrich), mounted with ProLong Gold antifade reagent (Thermo Fischer Scientific) and observed by fluorescence microscopy.

Multicolour experiment involving the detection of LDs, actin microfilaments and DNA: After incubating HeLa cells with the corresponding dye (75 nM for 1 h), the cells on coverslips were fixed in 4% PFA for 20 min at 4 °C, washed three times with PBS (5 min each), permeabilized and blocked as described above. F-actin was visualized by incubation with Alexa Fluor® 555 Phalloidin (Thermo Fisher Scientific) solution (1:200) at 37 °C in a wet chamber for 30 min. Finally, cells were washed three times with PBS, counterstained with Hoechst-33258 and mounted with Prolong Gold antifade reagent as described above.

1.10. Microscopy

Fluorescence microscopy images were acquired by using an Olympus BX63 automated fluorescence microscope equipped with a CoolLED's pE-300 light source (CoolLED Ltd., Andover, UK) and an Olympus DP74 digital camera (Olympus, Center Valley, PA, USA). Confocal microscopy images were acquired by using a SP8 confocal multispectral system (Leica Microsystems) with white laser (WLL2) for excitation, time gating hybrid detectors for fluorescence emission, HC PlanApo CS2 63x/1.20 N.A. water objective, and zoom 0.75x. The excitation and emission wavelengths selected to visualize the probes were: BODIPY **2** (excitation: 488 and 560 nm; emission: 500-540 nm and 570-648 nm for green or red images, respectively); BODIPY **6** (excitation: 488 nm; emission: 500-540 and 565-615 nm for green and red images, respectively); BODIPY **9** (excitation: 560 nm; emission: 570-620 nm). DIC microscopy images were acquired by using the same microscope used for confocal microscopy.

2. Supplementary figures.

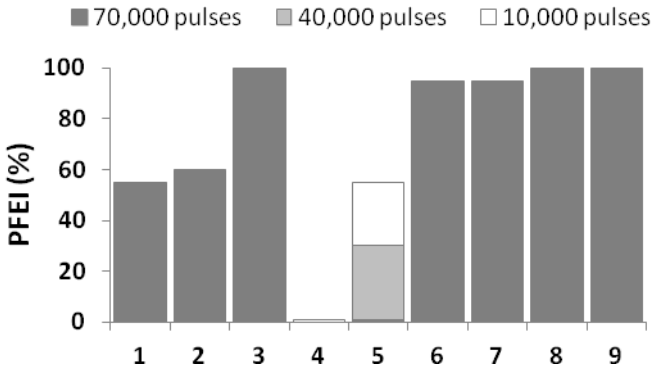

Fig. S1. Different photostability of **1-9**, in terms of PFEI, in ethyl acetate solution (10^{-3} M) after 10,000 (white bars), 40,000 (grey bars) and 70,000 (black bars) pump pulses. PFEI is the percent laser-induced fluorescent emission intensity in ethyl acetate solution after n pumping laser pulses, referred to the initial intensity.

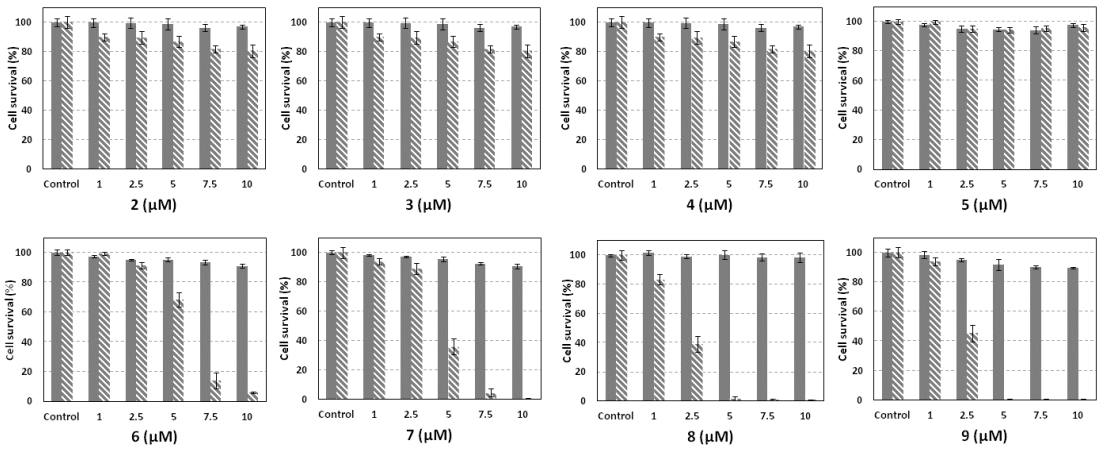

Fig. S2. HeLa cells survival after incubating with different concentrations of **2**-**9** for 24 h in absence of light (solid bars) or including subsequent irradiation with a 10.3 J/cm^2 dose of green light (518±10 nm; stripped bars). Cell viability was evaluated by MTT assay 24 h after the treatments. Data correspond to mean ± S.D. values from at least six different experiments. Statistically significant differences are labelled as * ($p<0.001$) for comparisons between groups using one-way ANOVA (all groups *vs.* control; differences are not statistically significant when it is not indicated).

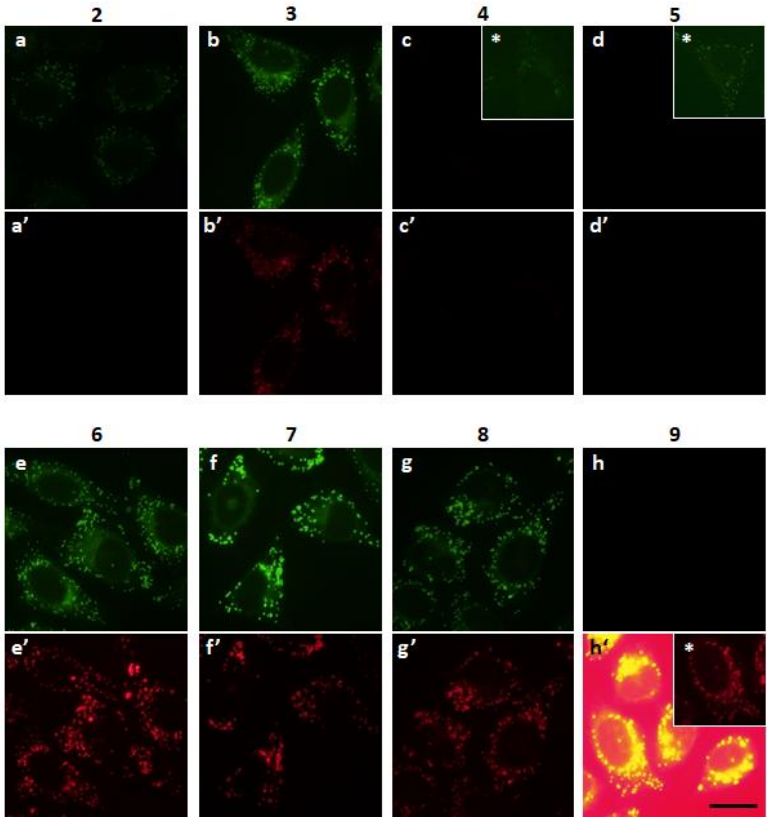

Fig. S3. Differential sharp in LD bioimaging using **2-9**. HeLa cells were incubated with the corresponding dye (5 µM for 24 h), and visualized using the blue (495/525; exposure time = 30.9 ms) (a-h) or green (545/620; exposure time = 400.0 ms) (a'-h') microscope channel, to obtain green and red images, respectively. *300.0 ms and 6.5 ms were respectively used for **5** and **9**. Scale bar: 20 µm.

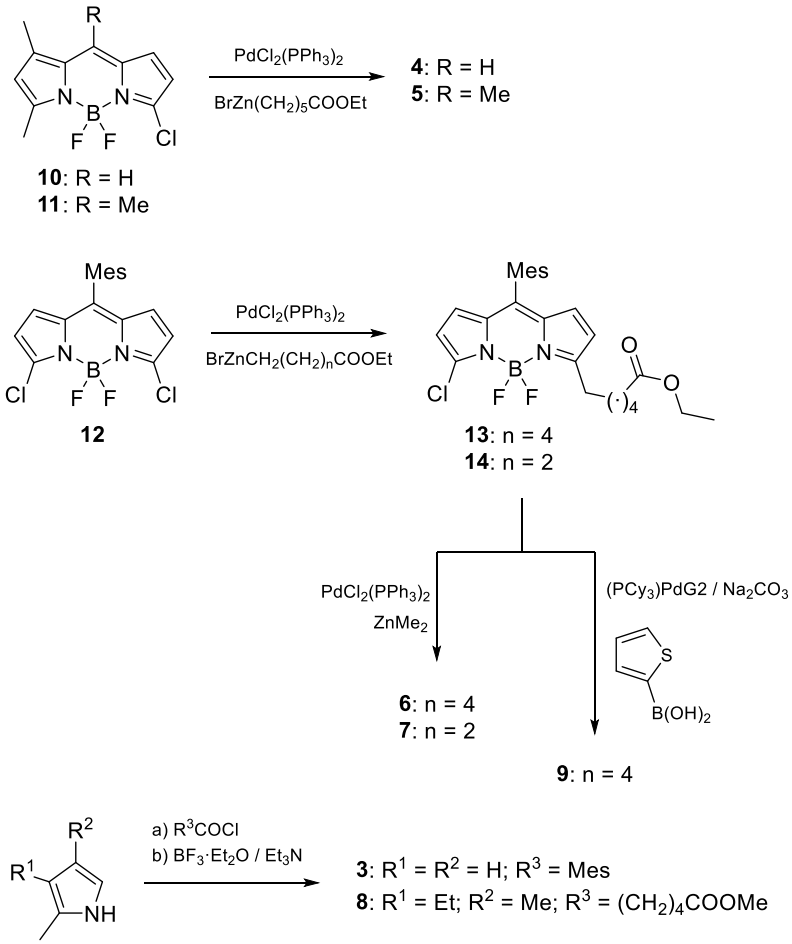

Fig. S4. Synthesis of BODIPYs **3**-**9**. Mes: Mesityl; $(PCy_3)PdG2$: Chloro[(tricyclohexylphosphine)-2-(2′-aminobiphenyl)]palladium(II).

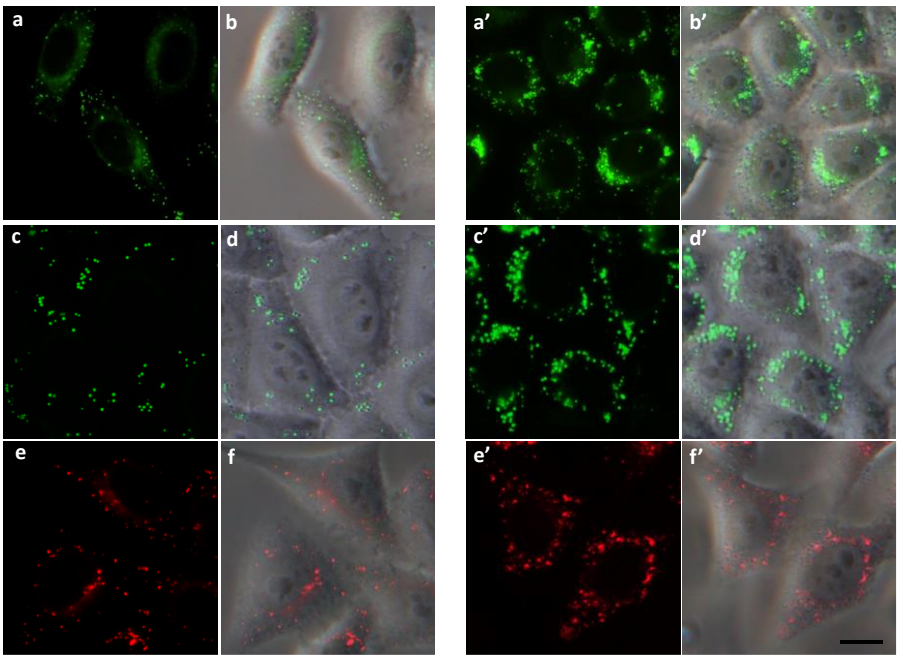

Fig. S5. Bioimaging using **2** (a-b), **6** (c-d) and **9** (e-f) under standard incubation conditions (a-f), or after treating the cells with sunflower oil before said incubation (a'-f'). The enhanced volume of the detected spherical organelles demonstrates that they are LDs. Scale bar 10 µm.

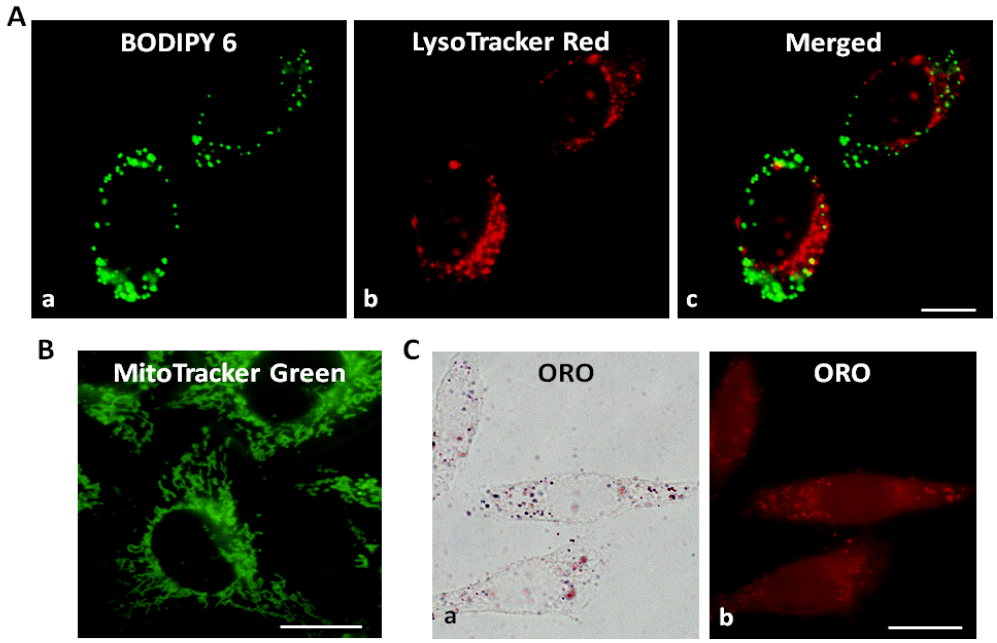

Fig. S6. Subcellular co-localization experiments. A: Fluorescence bioimaging of HeLa cells showing the localization of BODIPY **6** by using the blue microscope channel (a), the localization of LysoTracker® Red (lysosome probe) by using the green microscope channel (b), the corresponding merged image (c) demonstrate that no co-localization occurs between the green **6** signal (green) and lysosomes labeled with LysoTracker® Red. Scale bar: 5 μm. B: Fluorescence bioimaging of HeLa cells showing the localization of MitoTracker® Green (mitochondria probe) by using the blue microscope channel (note the typical morphology of the mitochondrial network), which is completely different from the fluorescent pattern obtained by using **6**. C: HeLa cells stained with Oil Red O (ORO) revealing "red" LDs under bright field microscopy (a) and fluorescence microscopy (b). Note that LDs stained with ORO show a similar size, morphology and distribution pattern to that obtained by using **6**. Using **2** or **9** instead of **6** in similar experiments gave place to similar results.

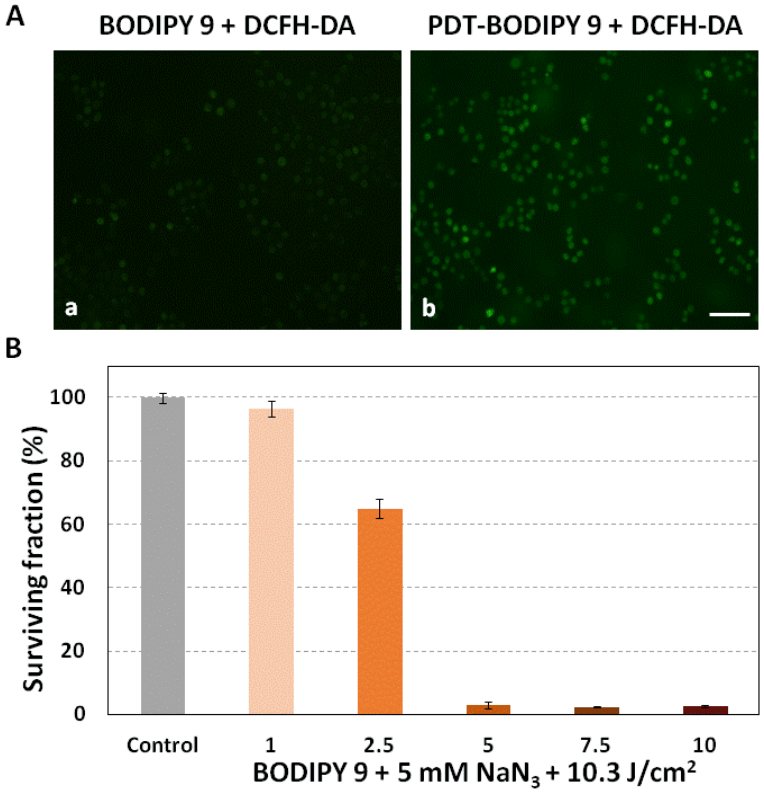

Fig. S7. Cellular oxidative stress detection assays. A: Qualitative characterization of ROS generation in the LD-**9** system by DCFH-DA assay. Fluorescence images of HeLa cells after incubation with **9** in the dark (a) and after irradiation (b). Scale bar: 100 µm. B: Cell survival (%) of HeLa cells exposed to **9** in presence of 5 mM NaN_3 (singlet oxygen quencher) and irradiated. HeLa cells were treated with 5 mM NaN_3 for 2 h before irradiation (10.3 J/cm^2). Values are the mean ± standard deviation of three replicate experiments. NaN_3 increased the rate of cell survival (*e.g.*, from 45% to 65 % when using 2.5 µM **9**), thus supporting the involvement of $^1O_2$ in the PDT activity. However, since cell damage is still produced, other ROS are also photogenerated, contributing to the final PDT activity.

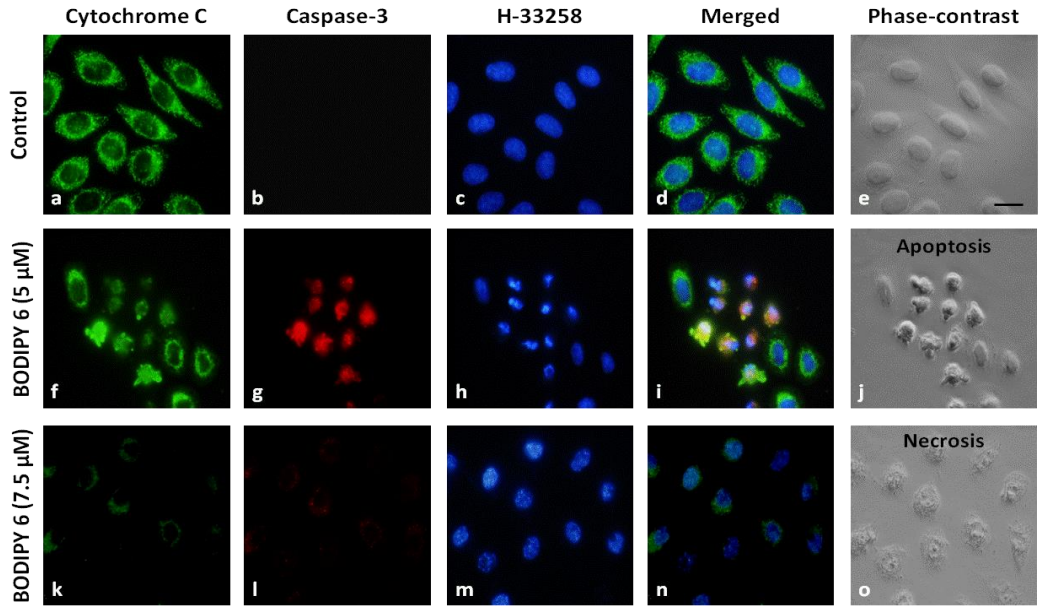

Fig. S8. Switching apoptosis vs. necrosis by changing **6** concentration in the PDT treatment. The identification of the type of cell death was carried out by immnunofluorescence for two proteins involved in apoptosis: Cytochrome c (green) and active Caspase-3 (red). Nuclei integrity was studied by DNA counterstaining with Hoechst-33258 (blue). In addition, morphological changes were examined by phase-contrast microscopy. Untreated (control) HeLa cells showed mitochondrial cytochrome-c signal (a), negative expression of active caspase-3 (b), non-condensed chromatin (c), and characteristic HeLa cell morphology (d). HeLa cells after photodynamic treatment with 5 µM **6** showed release of Cytochrome c from mitochondria to cytosol (f), intense red signal from activated Caspase-3 (g), chromatin condensation and nuclear fragmentation (h and i), cell shrinkage and appearance of membrane bubbles (j). The last features are typical of apoptotic death. On the other hand, after photodynamic treatments with 7.5 µM **6**, release of cytochrome c (k) and active caspase-3 (l) were not detected, nuclei show condensed chromatin in "patches" (m and n), and the observed morphological alteration consists in loss of cell membrane integrity (o). These features are typical of necrotic death.

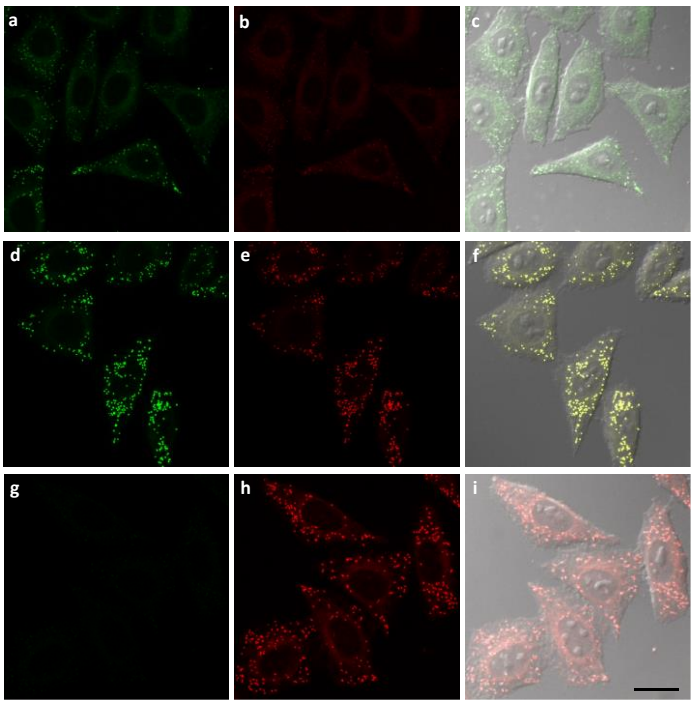

Fig. S9. Differential behaviour of **2** (a-c), **6** (d-f) and **9** (g-i) as nanomolar probes (cells incubated with 75 nM dye for 1 h) for visualizing LDs in living HeLa cells using the blue (a, d and g) or green (b, e and h) microscope channels, and by merging the corresponding green, red and DIC images (c, f and i). No alteration of the cell morphology supports lack of dye cytotoxicity under the used experimental conditions. Scale bar: 20 µm.

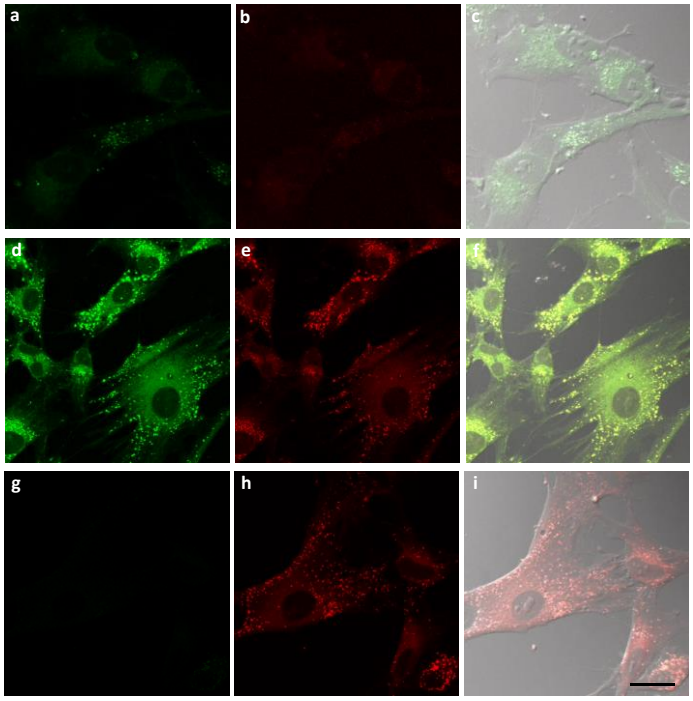

Fig. S10. Differential behaviour of **2** (a-c), **6** (d-f) and **9** (g-i) as nanomolar probes (cells incubated with 75 nM dye for 1 h) for visualizing LDs in living Hs68 cells using the blue (a, d and g) or green (b, e and h) microscope channels, and by merging the corresponding green, red and DIC images (c, f and i). No alteration of the cell morphology supports lack of dye cytotoxicity under the used experimental conditions. Scale bar: 20 µm.

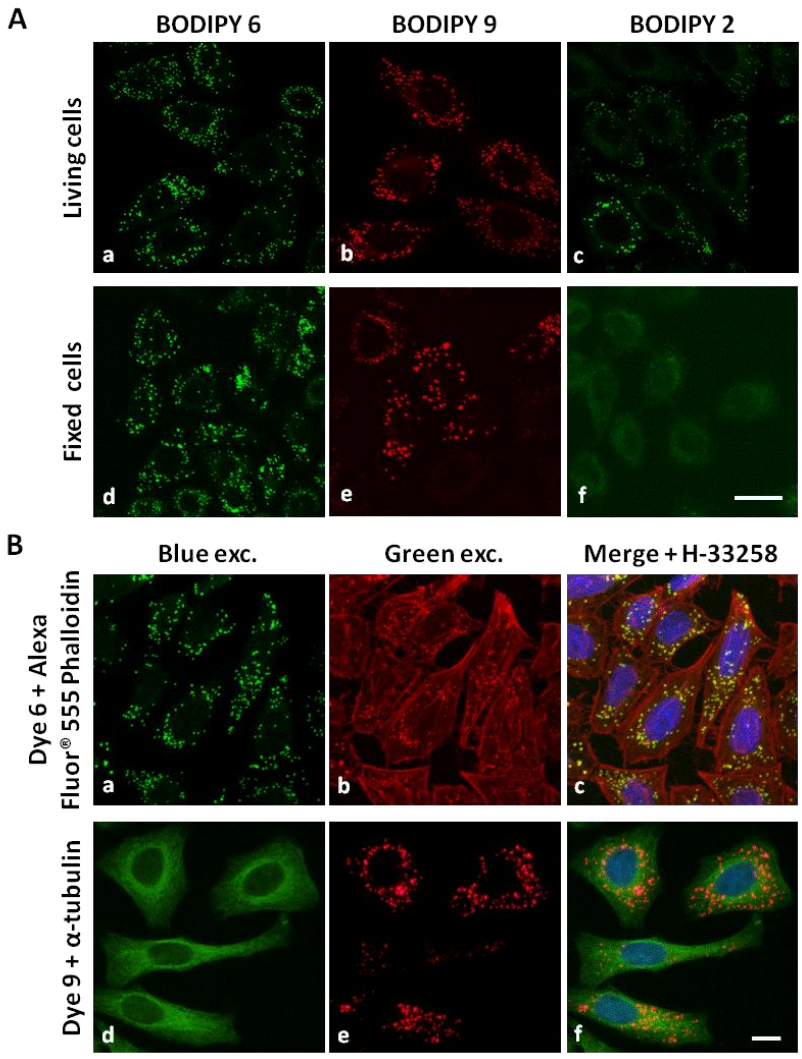

Fig. S11. Fluorescent signal remained unaltered after the fixation process of HeLa cells. A: Bioimaging of living cells incubated with **6** (a), **9** (b) or **2** (c), and bioimaging of the same cells after 15 min of 4% PFA fixation (d-f). Fluorescent detection of LDs in fixed cells was only possible by using **6** or **9**. Scale bar 20 µm. B (up): Bioimaging of HeLa cells incubated with **6**, fixed, permeabilized with Triton X-100 and incubated with Alexa Fluor® 555 Phalloidin. LD detection using the blue microscope channel (a); actin-F detection using the green microscope channel (b); simultaneous detection of actin filaments, LDs and Hoechst-33258 counterstained nuclei by merging the corresponding images obtained by blue, green and UV excitation (c). B (down): Bioimaging of HeLa cells incubated with **9,** fixed and immunolabeled for α-tubulin (microtubule detection). Microtubules detection using the blue microscope channel (d); LD detection using the green microscope channel (e); simultaneous detection of microtubules, LDs and Hoechst-33258 counterstained nuclei by merging the corresponding images obtained by blue, green and UV excitation (f). Scale bar: 10 µm.

3. Supplementary table

Table S1. Fluorescence signatures of **2-9** in diluted (*ca.* 0.5 x 10^{-6} M) ethyl acetate solution. Maximum absorption (λ_{ab}) and maximum fluorescence (λ_{fl}) wavelengths, Stokes shifts ($\Delta\nu$) and fluorescence quantum yields (ϕ).

BODIPY	λ_{ab} (nm)	λ_{fl} (nm)	$\Delta\nu$ (cm^{-1})	ϕ
2 [a]	494	504	400	0.85
3	498	516	700	0.80
4	510	518	303	0.77
5	496	506	398	0.87
6	509	519	379	0.80
7	514	524	371	0.73
8	525	538	460	0.70
9	568	580	364	0.60

[a] Data collected from ref. 1.

4. Synthesis and characterization

BODIPYs **1** and **2** (see Fig. S1 in ESI) are commercially available (laser grade; purity > 99%), and were used as received. 8-Mesity-3,5-dimethylBODIPY (**3**,[8] see Fig. 1 in the main text), 5-chloro-1,3-dimethylBODIPY (**10**,[9] see Fig. S5), 5-chloro-1,3,8-trimethylBODIPY (**11**,[9] see Fig. S5) and 3,5-dichloro-8-mesitylBODIPY (**12**,[10] see Fig. S5) were synthesized by the corresponding described methods.

4.1. General procedure for Negishi reactions

The corresponding haloBODIPY (0.10-0.35 mmol), $PdCl_2(PPh_3)_2$ (10 mol%) and dry toluene (2 mL) were placed into a Schlenk tube capped with a rubber septum, under argon atmosphere. This tube was previously air-evacuated and backfilled with argon (this sequence is repeated three times). Then, the corresponding organozinc reagent (0.26-1.75 mmol) was drop-wised added over the mixture and the resulting reaction mixture stirred at r.t. for 1-6 h. The reaction progress was monitored by thick layer chromatography (TLC) on silica gel. Once the reaction was monitored as finalized, the mixture was filtered (CH_2Cl_2 was used for elution and washing), and the obtained solution submitted to solvent evaporation under vacuum. The obtained residue was purified by flash chromatography on silica gel.

4.2. Synthesis of 4

According to above described general procedure for Negishi reactions, **10**[9] (40 mg, 0.16 mmol), $PdCl_2(PPh_3)_2$ (11 mg, 0.016 mmol) and 0.5 M $BrZn(CH_2)_5COOEt$ in THF (1.9 mL, 0.95 mmol) in dry toluene (2 mL) were reacted for 3 h. Flash chromatography using hexane/EtOAc (98:2) afforded **4** (50 mg, 86%) as a brown solid. ^{1}H NMR (700 MHz, $CDCl_3$) δ 7.06 (s, 1H, CH), 6.90 (d, J = 4.2 Hz, 1H, CH), 6.27 (d, J = 4.2 Hz, 1H, CH), 6.09 (s, 1H, CH), 4.12 (q, J = 7.0 Hz, 2H, CH_2O), 2.97 (t, J = 7.7 Hz, 2H, CH_2), 2.55 (s, 3H, CH_3), 2.31 (t, J = 7.7 Hz, 2H, CH_2), 2.24 (s, 3H, CH_3), 1.75 (quint, J = 7.7 Hz, 2H, CH_2), 1.69 (quint, J = 7.7 Hz, 2H, CH_2), 1.46 (quint, J = 7.7 Hz, 2H, CH_2), 1.25 (t, J = 7.0 Hz, 3H, CH_3) ppm; ^{13}C NMR (176 MHz, $CDCl_3$) δ 173.8 (COO), 160.3 (C), 159.2 (C), 143.0 (C), 134.7 (C), 133.3 (C), 128.4 (CH), 123.5 (CH), 120.0 (CH), 116.8 (CH), 60.2 (CH_2O), 34.3 (CH_2), 29.0 (CH_2), 28.5 (CH_2), 28.3 (CH_2), 24.8 (CH_2), 14.9 (CH_3), 14.3 (CH_3), 11.3 (CH_3) ppm; FTIR ν 2925, 2844,

1723, 1570, 1311, 1145, 986 cm^{-1}; HRMS-EI *m/z* 362.1969 (362.1977 calcd for $C_{19}H_{25}BF_2N_2O_2$).

4.3. Synthesis of 5

According to above described general procedure for Negishi reactions, **11**[9] (93 mg, 0.35 mmol), $PdCl_2(PPh_3)_2$ (24.6 mg, 0.035 mmol) in dry toluene (2 mL) and 0.5 M $BrZn(CH_2)_5CO_2Et$ in THF (3.5 mL, 1.75 mmol) were reacted for 6 h. Flash chromatography using hexane/CH_2Cl_2 (5:5) afforded unaltered **11** (12 mg, 15%), and **5** (80 mg, 61%) as a brown solid. ^{1}H NMR (700 MHz, $CDCl_3$) δ 7.09 (d, *J* = 4.2 Hz, 1H, CH), 6.26 (d, *J* = 4.2 Hz, 1H, CH), 6.08 (s, 1H, CH), 4.12 (q, *J* = 7.0 Hz, 2H, CH_2O), 2.96 (t, *J* = 7.7 Hz, 2H, CH_2), 2.54 (s, 3H, CH_3), 2.50 (s, 3H, CH_3), 2.38 (s, 3H, CH_3), 2.30 (t, *J* = 7.7 Hz, 2H, CH_2), 1.74 (quint, *J* = 7.7 Hz, 2H, CH_2), 1.69 (quint, *J* = 7.7 Hz, 2H, CH_2), 1.45 (quint, *J* = 7.7 Hz, 2H, CH_2), 1.25 (t, *J* = 7.0 Hz, 3H, CH_3) ppm; ^{13}C NMR (176 MHz, $CDCl_3$) δ 173.8 (COO), 158.7 (C), 156.5 (C), 142.7 (C), 140.4 (C), 134.3 (C), 132.7 (C), 125.7 (CH), 121.7 (CH), 115.9 (CH), 60.2 (CH_2O), 34.3 (CH_2), 29.0 (CH_2), 28.4 (CH_2), 28.3 (CH_2), 24.8 (CH_2), 16.6 (CH_3), 16.4 (CH_3), 14.7 (CH_3), 14.3 (CH_3) ppm; FTIR ν 2926, 2857, 1730, 1561, 1301, 1150, 987 cm^{-1}; HRMS-EI *m/z* 376.2130 (376.2134 calcd for $C_{20}H_{27}BF_2N_2O_2$).

4.4. Synthesis of 13

According to above described general procedure for Negishi reactions, **12**[10] (50 mg, 0.13 mmol), $PdCl_2(PPh_3)_2$ (9 mg, 0.013 mmol) and 0.5 M $BrZn(CH_2)_5COOEt$ in THF (1 mL, 0.528 mmol) in dry toluene (2 mL) were reacted for 1.5 h. Flash chromatography using hexane/EtOAc (95:5) afforded unaltered **12** (15 mg, 30%), and **13** (40 mg, 62%) as a brown solid. ^{1}H NMR (700 MHz, $CDCl_3$) δ 6.93 (s, 2H, 2CH), 6.62 (d, *J* = 4.2 Hz, 1H, CH), 6.44 (d, *J* = 4.2 Hz, 1H, CH), 6.36 (d, *J* = 4.2 Hz, 1H, CH), 6.26 (d, *J* = 4.2 Hz, 1H, CH), 4.12 (q, *J* = 7.0 Hz, 2H, CH_2O), 3.07 (t, *J* = 7.7 Hz, 2H, CH_2), 2.34 (s, 3H, CH_3), 2.32 (t, *J* = 7.7 Hz, 2H, CH_2), 2.09 (s, 6H, $2CH_3$), 1.79 (quint, *J* = 7.7 Hz, 2H, CH_2), 1.70 (quint, *J* = 7.7 Hz, 2H, CH_2), 1.49 (quint, *J* = 7.7 Hz, 2H, CH_2), 1.25 (t, *J* = 7.0 Hz, 3H, CH_3) ppm; ^{13}C NMR (176 MHz, $CDCl_3$) δ 173.7 (COO), 166.3 (C), 142.9 (C), 140.2 (C), 138.8 (C), 136.6 (C), 135.6 (C), 133.0 (C), 131.5 (CH), 129.1 (C), 128.2 (CH), 127.4 (CH), 120.0 (CH), 116.8 (CH), 60.3 (CH_2O), 34.2 (CH_2), 29.1 (CH_2), 29.0 (CH_2), 28.1 (CH_2), 24.8 (CH_2), 21.1 (CH_3), 20.0

(CH_3), 14.3 (CH_3) ppm; FTIR ν 2928, 2862, 1730, 1562, 1408, 1329, 1267, 1102, 1045, 970 cm^{-1}; HRMS-EI *m/z* 486.2051 (486.2057 calcd for $C_{26}H_{30}BClF_2N_2O_2$).

4.5. Synthesis of 6

According to above described general procedure for Negishi reactions, **13** (52 mg, 0.11 mmol), $PdCl_2(PPh_3)_2$ (8 mg, 0.011 mmol) and 1.2 M $ZnMe_2$ in toluene (0.22 mL, 0.265 mmol) in dry toluene (2 mL) were reacted for 1 h. Flash chromatography using hexane/EtOAc (95:5) afforded **6** (37 mg, 75%) as a brown solid. ^{1}H NMR (300 MHz, $CDCl_3$) δ 6.92 (s, 2H, 2CH), 6.48 (d, *J* = 4.2 Hz, 1H, CH), 6.46 (d, *J* = 4.2 Hz, 1H, CH), 6.24 (d, *J* = 4.2 Hz, 1H, CH), 6.19 (d, *J* = 4.2 Hz, 1H, CH), 4.12 (q, *J* = 7.2 Hz, 2H, CH_2O), 3.03 (t, *J* = 7.8 Hz, 2H, CH_2), 2.63 (s, 3H, CH_3), 2.34 (s, 3H, CH_3), 2.32 (t, *J* = 7.5 Hz, 2H, CH_2), 2.09 (s, 6H, $2CH_3$), 1.83-1.66 (m, 4H, $2CH_2$), 1.54-1.44 (m, 2H, CH_2), 1.25 (t, *J* = 7.2 Hz, 3H, CH_3) ppm; ^{13}C NMR (75 MHz, $CDCl_3$) δ 173.7 (COO), 162.0 (C), 157.5 (C), 142.4 (C), 138.3 (C), 136.6 (C), 134.7 (C), 134.5 (C), 130.1 (C), 129.0 (CH), 128.9 (CH), 128.0 (CH), 119.3 (CH), 117.6 (CH), 60.2 (CH_2O), 34.3 (CH_2), 29.1 (CH_2), 28.7 (CH_2), 28.2 (CH_2), 24.8 (CH_2), 21.1 (CH_3), 20.0 (CH_3), 14.9 (CH_3), 14.3 (CH_3) ppm; FTIR ν 2926, 2860, 1733, 1560, 1272, 1142, 1125, 1089, 999 cm^{-1}; HRMS-EI *m/z* 466.2597 (466.2603 calcd for $C_{27}H_{33}BF_2N_2O_2$).

4.6. Synthesis of 14

According to above described general procedure for Negishi reactions, **12**[10] (50 mg, 0.13 mmol), $PdCl_2(PPh_3)_2$ (9 mg, 0.013 mmol) and 0.5 M $BrZn(CH_2)_3COOEt$ in THF (0.78 mL, 0.39 mmol) in dry toluene (2 mL) were reacted for 1 h. Flash chromatography using hexane/EtOAc (98:2) afforded unaltered **12** (7 mg, 14%), and **14** (39 mg, 65%) as an orange solid. ^{1}H NMR (700 MHz, $CDCl_3$) δ 6.93 (s, 2H, 2CH), 6.62 (d, *J* = 4.2 Hz, 1H, CH), 6.46 (d, *J* = 4.2 Hz, 1H, CH), 6.39 (d, *J* = 4.2 Hz, 1H, CH), 6.27 (d, *J* = 4.2 Hz, 1H, CH), 4.14 (q, *J* = 7.0 Hz, 2H, CH_2O), 3.11 (t, *J* = 7.7 Hz, 2H, CH_2), 2.45 (t, *J* = 7.7 Hz, 2H, CH_2), 2.34 (s, 3H, CH_3), 2.11 (quint, *J* = 7.7 Hz, 2H, CH_2), 2.09 (s, 6H, $2CH_3$), 1.26 (t, *J* = 7.0 Hz, 3H, CH_3) ppm; ^{13}C NMR (176 MHz, $CDCl_3$) δ 173.1 (COO), 164.9 (C), 143.3 (C), 140.7 (C), 138.8 (C), 136.6 (C), 135.6 (C), 133.2 (C), 131.5 (CH), 129.0 (C), 128.2 (CH), 127.8 (CH), 119.9 (CH), 117.1 (CH), 60.5 (CH_2O), 33.8 (CH_2), 28.3 (CH_2), 23.7 (CH_2), 21.1 (CH_3), 20.0 (CH_3), 14.2 (CH_3) ppm; FTIR ν 2923, 2852, 1735, 1569, 1539, 1411, 1348, 1332, 1271, 1186,

1111, 1048, 993, 973 cm^{-1}; HRMS-EI *m/z* 458.1738 (458.1744 calcd. for $C_{24}H_{26}BClF_2N_2O_2$).

4.7. Synthesis of 7

According to above described general procedure for Negishi reactions, **14** (46 mg, 0.10 mmol), $PdCl_2(PPh_3)_2$ (7 mg, 0.010 mmol) and 1.2 M $ZnMe_2$ in toluene (0.5 mL, 0.5 mmol) in dry toluene (2 mL) were reacted for 4 h. Flash chromatography using hexane/Et_2O (98:2) afforded **7** (30 mg, 67%) as an orange solid, and unaltered **14** (13 mg, 28%). ^{1}H NMR (300 MHz, $CDCl_3$) δ 6.92 (s, 2H, 2CH), 6.48 (d, *J* = 4.2 Hz, 2H, 2CH), 6.27 (d, *J* = 4.2 Hz, 1H, CH), 6.20 (d, *J* = 4.2 Hz, 1H, CH), 4.15 (q, *J* = 7.2 Hz, 2H, CH_2O), 3.07 (t, *J* = 7.8 Hz, 2H, CH_2), 2.63 (s, 3H, CH_3), 2.45 (t, *J* = 7.8 Hz, 2H, CH_2), 2.34 (s, 3H, CH_3), 2.15-2.05 (m, 8H, CH_2 and $2CH_3$), 1.27 (t, *J* = 7.2 Hz, 3H, CH_3) ppm; ^{13}C NMR (75 MHz, CDCl3) δ 173.3 (COO), 160.5 (C), 158.0 (C), 142.7 (C), 138.4 (C), 136.6 (C), 134.8 (C), 134.4 (C), 130.1 (C), 129.3 (CH), 128.9 (CH), 128.0 (CH), 119.7 (CH), 117.6 (CH), 60.4 (CH_2O), 34.0 (CH_2), 28.1 (CH_2), 23.8 (CH_2), 21.1 (CH_3), 20.0 (CH_3), 15.0 (CH_3), 14.3 (CH_3) ppm; FTIR ν 2925, 2855, 1735, 1564, 1439, 1274, 1132, 1011 cm^{-1}; HRMS-EI *m/z* 438.2285 (438.2290 calcd for $C_{25}H_{29}BF_2N_2O_2$).

4.8. Synthesis of 8

To a solution of methyl 6-chloro-6-oxohexanoate* (175 mg, 0.97 mmol) in CH_2Cl_2 (15 mL) was added, under argon atmosphere, 3-ethyl-2,4-dimethylpyrrole (0.33 mL, 2.44 mmol), and the mixture was refluxed for 3 h. After cooling down to r.t., Et_3N (0.7 mL, 4.88 mmol) and $BF_3{\cdot}Et_2O$ (0.6 mL, 4.88 mmol) were added, and stirring maintened for 2 h. Finally, the solvent was removed by vacuum distillation, and the obtained residue solved in EtOAc. The obtained solution was washed with 10% aq HCl and H_2O. The organic layer was dried over Na_2SO_4, filtered and concentrated to dryness. The crude product was purified by flash chromatography, using silica gel and hexane/$CHCl_3$ (95:5), to afford **8** (120 mg, 30%) as an orange solid. ^{1}H NMR (300 MHz, $CDCl_3$) δ 3.67 (s, 3H, CH_3O), 3.03-2.98 (m, 2H, CH_2), 2.49 (s, 6H, $2CH_3$), 2.40 (t, *J* = 7.2 Hz, 2H, CH_2), 2.40 (q, *J* = 7.5 Hz, 4H, $2CH_2$), 2.33 (s, 6H, $2CH_3$), 1.88-1.78 (m, 2H, CH_2), 1.72-1.63 (m, 2H, CH_2), 1.04 (t, *J* = 7.5 Hz, 6H, $2CH_3$) ppm; ^{13}C NMR (75 MHz, $CDCl_3$) δ 173.7 (COO), 152.2 (C), 144.0 (C), 135.6 (C), 132.7 (C), 130.9 (C), 51.7 (CH_3O), 33.6 (CH_2), 31.2 (CH_2), 28.2 (CH_2), 25.3 (CH_2), 17.2 (CH_2), 14.9

(CH_3), 13.3 (CH_3), 12.4 (CH_3) ppm. FTIR ν 2925, 2855, 1741, 1548, 1472, 1331, 1264, 1198, 1071, 982 cm^{-1}; HRMS-EI *m/z* 418.3356 (418.3358 calcd for $C_{23}H_{33}BF_2N_2O_2$).

**Synthesis of methyl 6-chloro-6-oxohexanoate*: To a solution of 6-methoxy-6-oxohexanoic acid (0.012 mL, 0.11 mmol) in CH_2Cl_2 (2 mL) was added, under argon atmosphere, tionyl chloride (0.035 mL, 0.44 mmol), and the mixture was refluxed for 20 min. Then, the excess of tionyl chloride and the solvent were removed by vacuum distillation. The product was used without further purification.

4.9. Synthesis of 9

Chloro[(tricyclohexylphosphine)-2-(2′-aminobiphenyl)]palladium(II) ($(PCy_3)PdG2$; 1 mg, 0.002 mmol), 1 M Na_2CO_3 in H_2O (1 mL) and 2-thienylboronic acid (17 mg, 0.132 mmol) were added to a solution of **13** (21 mg, 0.044 mmol) in dry toluene (3 mL) under argon atmosphere, and the mixture stirred at 100 ºC for 4.5 h. The reaction progress was monitored by TLC. Once the reaction was tested as completed by TLC, the mixture was filtered (CH_2Cl_2 is used for elution and washing), and the obtained organic layer washed with H_2O, dried over $MgSO_4$, filtered and submitted to solvent evaporation under vacuum. Flash chromatography using hexane/CH_2Cl_2 (8:2) afforded **9** (12 mg, 50%) as a purple solid, and unaltered **13** (5 mg, 23%). ^{1}H NMR (700 MHz, $CDCl_3$) δ 8.14 (d, *J* = 3.5 Hz, 1H, CH), 7.45 (d, *J* = 4.9 Hz, 1H, CH), 7.18 (apparent t, *J* = 4.2 Hz, 1H, CH), 6.94 (s, 2H, 2CH), 6.67 (d, *J* = 4.2 Hz, 1H, CH), 6.53 (d, *J* = 4.2 Hz, 1H, CH), 6.51 (d, *J* = 4.9 Hz, 1H, CH), 6.31 (d, *J* = 4.2 Hz, 1H, CH), 4.12 (q, *J* = 7.0 Hz, 2H, CH_2O), 3.09 (t, *J* = 7.7 Hz, 2H, CH_2), 2.36 (s, 3H, CH_3), 2.35 (t, *J* = 7.0 Hz, 2H, CH_2), 2.12 (s, 6H, $2CH_3$), 1.79 (quint, *J* = 7.7 Hz, 2H, $2CH_2$), 1.71 (quint, *J* = 7.7 Hz, 2H, CH_2), 1.50 (quint, *J* = 7.7 Hz, 2H, CH_2), 1.25 (t, *J* = 7.0 Hz, 3H, CH_3) ppm; ^{13}C NMR (176 MHz, $CDCl_3$) δ 173.8 (COO), 163.2 (C), 149.3 (C), 141.8 (C), 138.4 (C), 136.8 (C), 136.3 (C), 134.9 (C), 134.4 (C), 130.5 (CH), 130.2 (C), 129.2 (CH), 128.9 (CH), 128.6 (CH), 128.5 (CH), 128.1 (CH), 119.6 (CH), 118.7 (CH), 60.2 (CH_2O), 34.2 (CH_2), 29.1 (CH_2), 28.8 (CH_2), 28.1 (CH_2), 24.8 (CH_2), 21.1 (CH_3), 20.0 (CH_3), 14.3 (CH_3) ppm; FTIR ν 2925, 2855, 1734, 1570, 1465, 1372, 1269, 1125, 1039 cm^{-1}; HRMS-EI *m/z* 534.2320 (534.2324 calcd. for ($C_{30}H_{33}BF_2N_2O_2S$).

5. ^{1}H NMR and ^{13}C NMR spectra

^{1}H NMR (700 MHz, $CDCl_3$) and ^{13}C NMR (176 MHz, $CDCl_3$) spectra of **4**

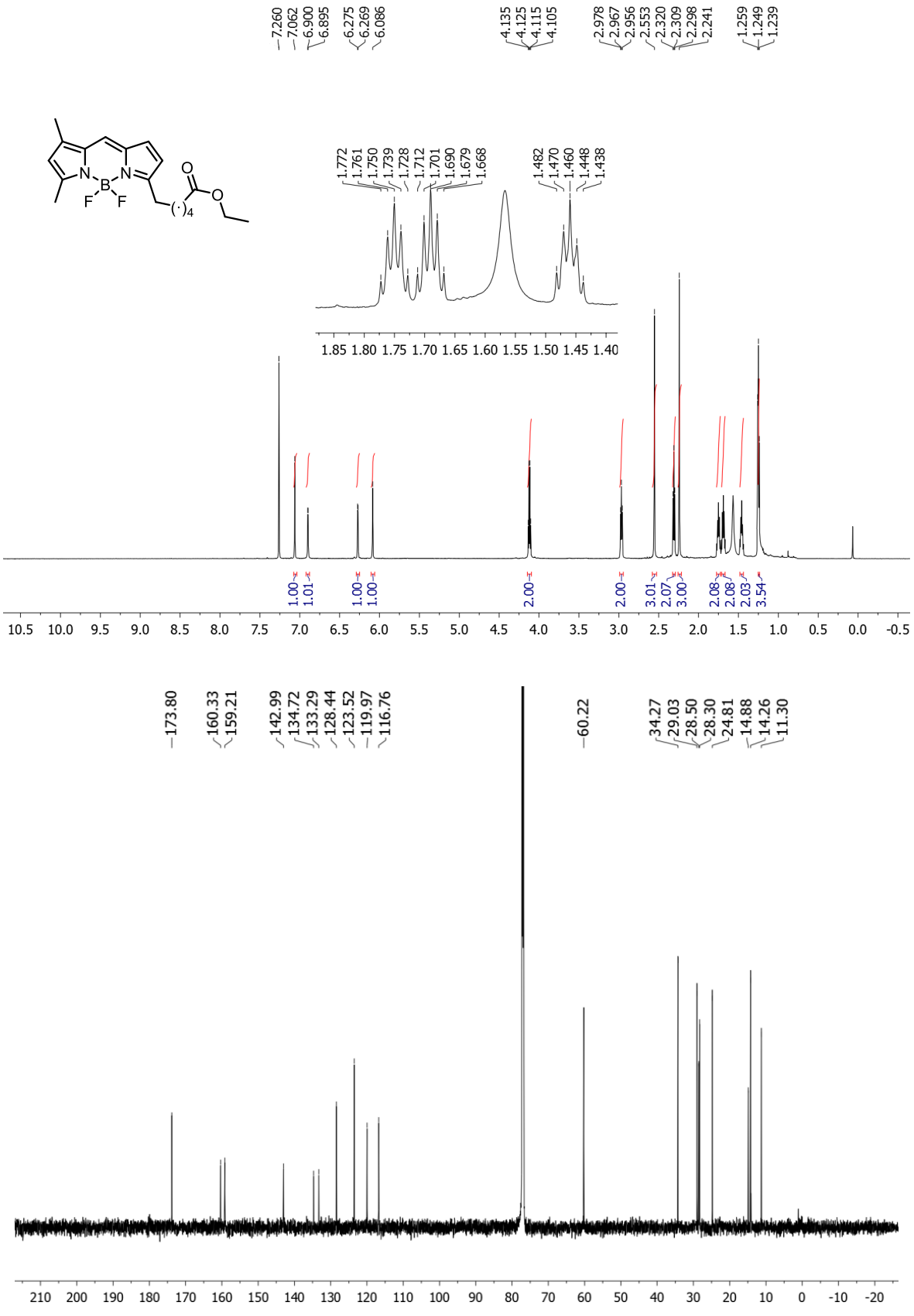

^{1}H NMR (700 MHz, $CDCl_3$) and ^{13}C NMR (176 MHz, $CDCl_3$) spectra of **5**

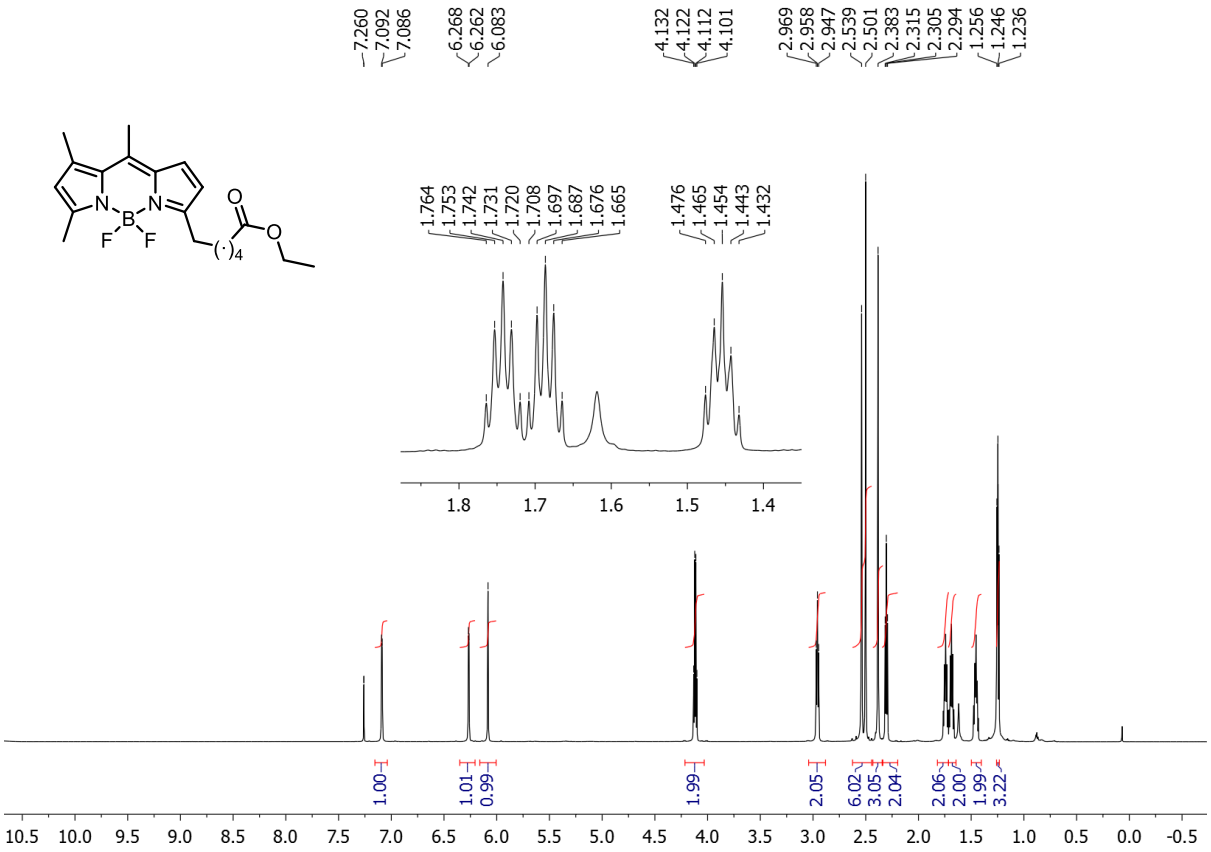

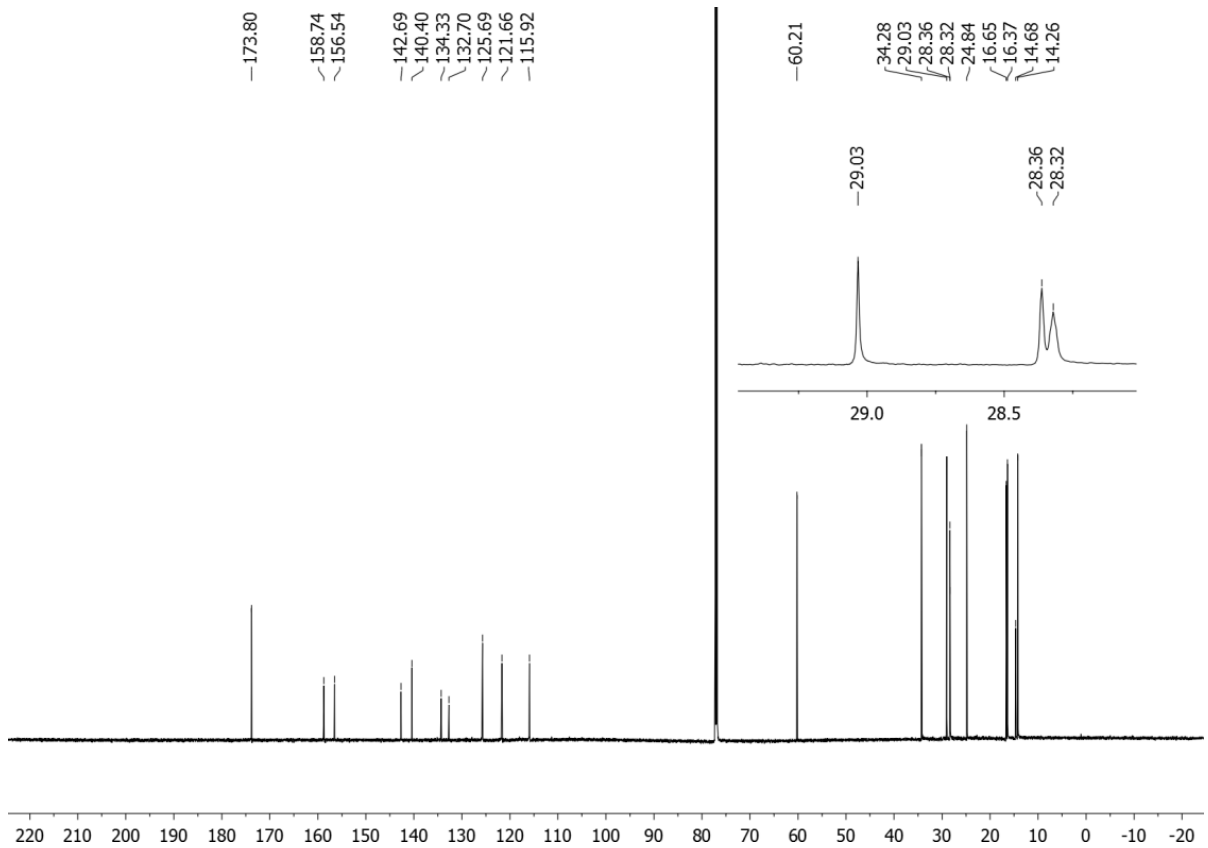

^{1}H NMR (700 MHz, $CDCl_3$) and ^{13}C NMR (176 MHz, $CDCl_3$) spectra of **13**

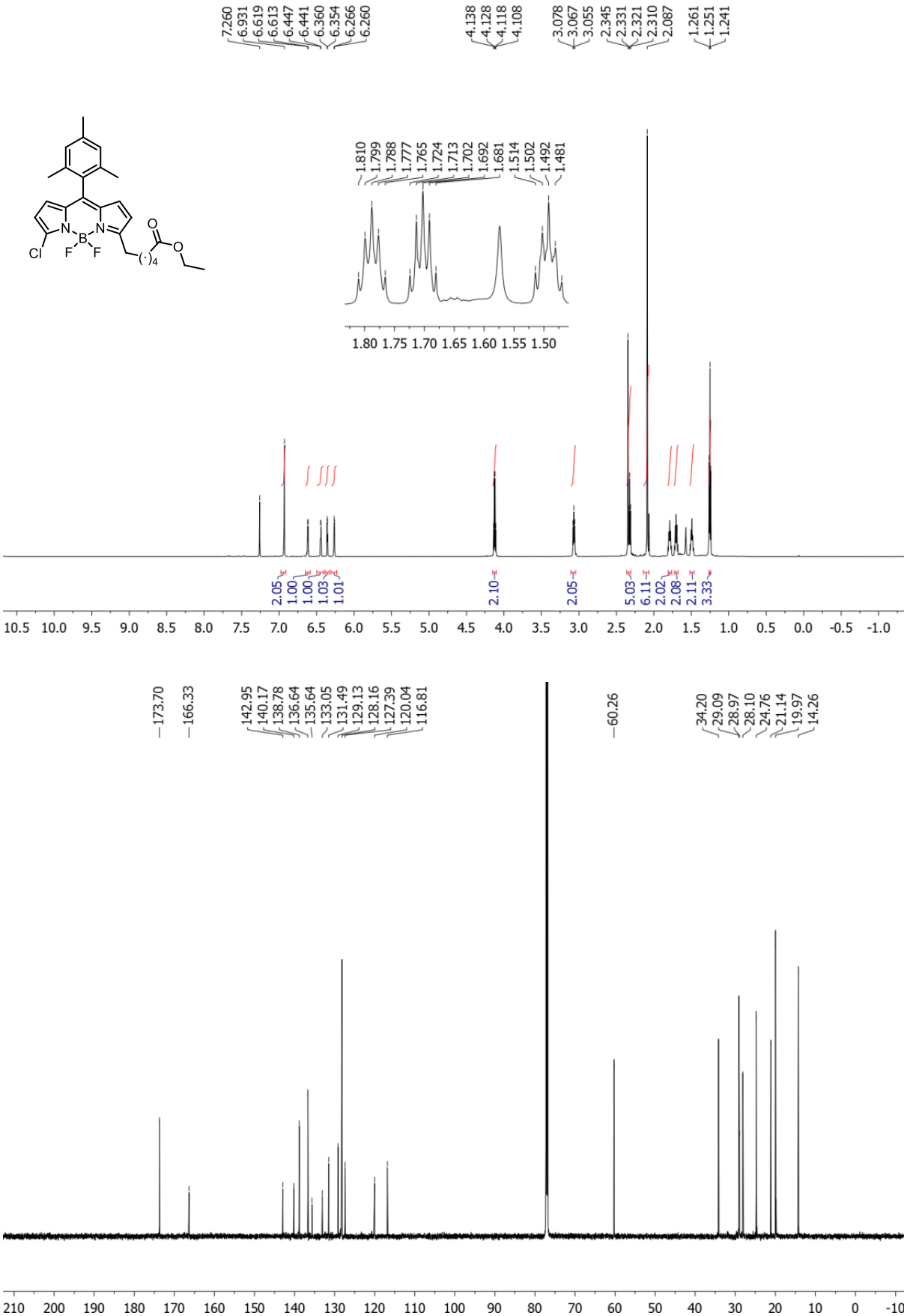

^{1}H NMR (300 MHz, $CDCl_3$) and ^{13}C NMR (75 MHz, $CDCl_3$) spectra of **6**

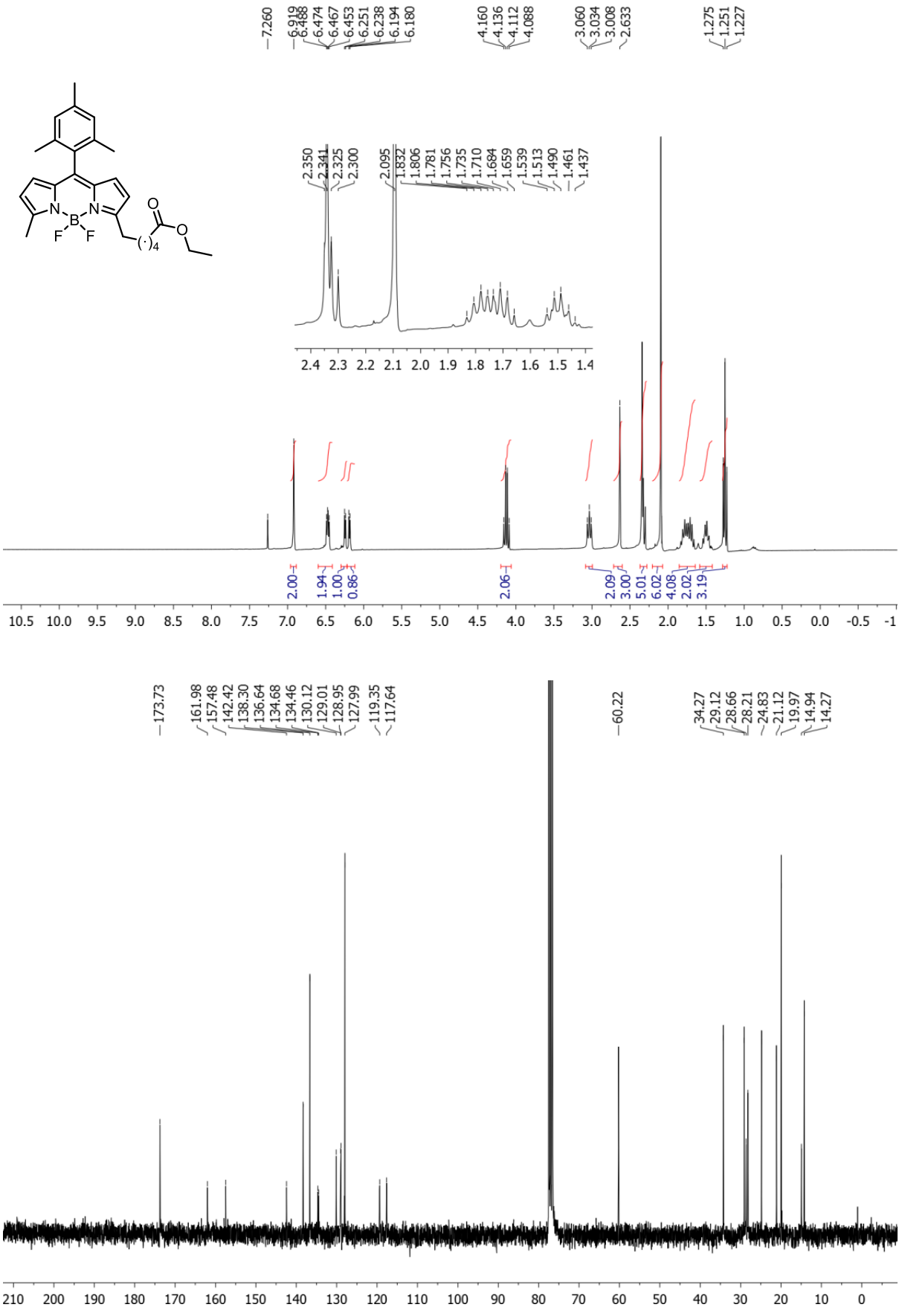

^{1}H NMR (700 MHz, $CDCl_3$) and ^{13}C NMR (176 MHz, $CDCl_3$) spectra of **14**

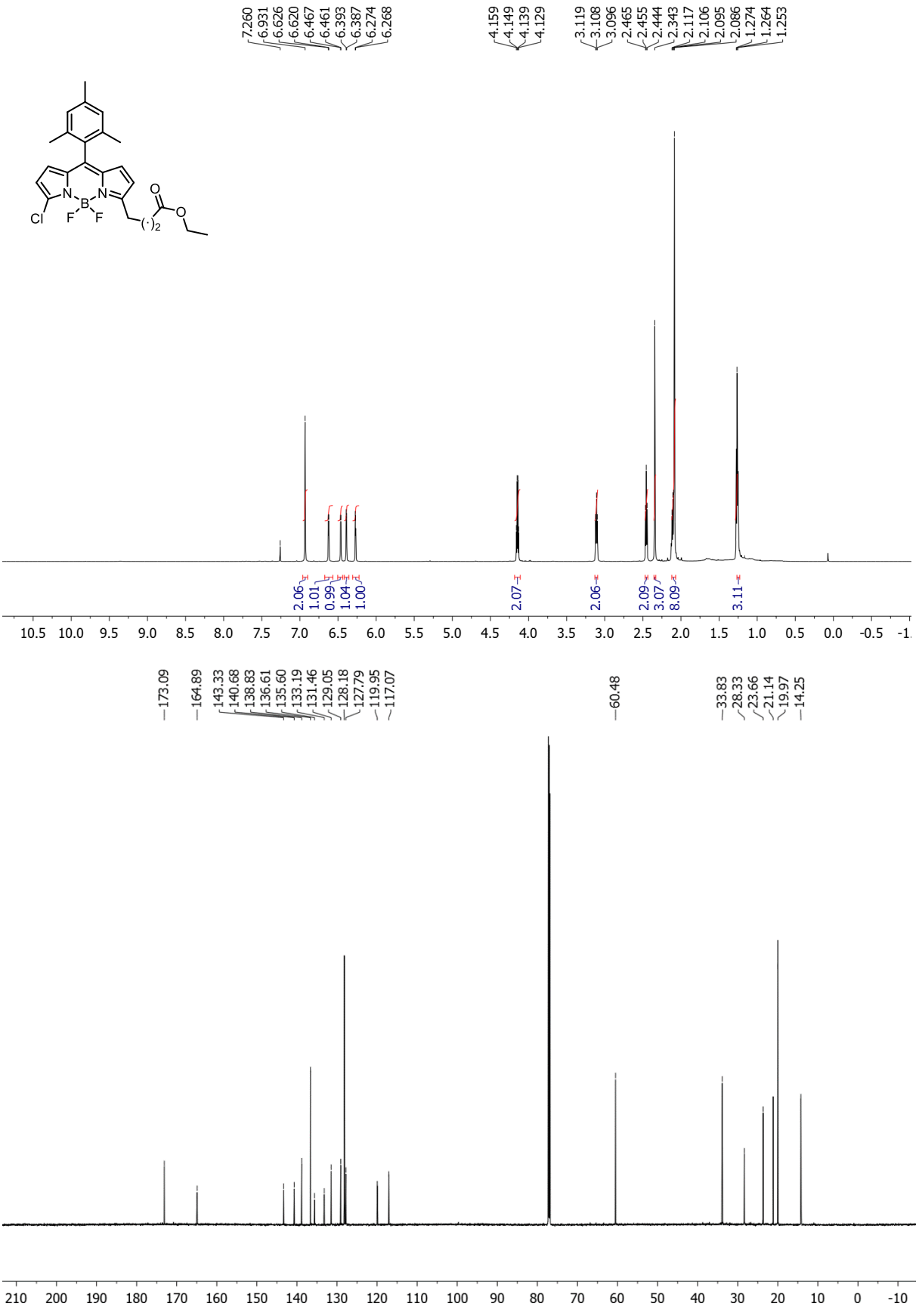

^{1}H NMR (300 MHz, $CDCl_3$) and ^{13}C NMR (75 MHz, $CDCl_3$) spectra of **7**

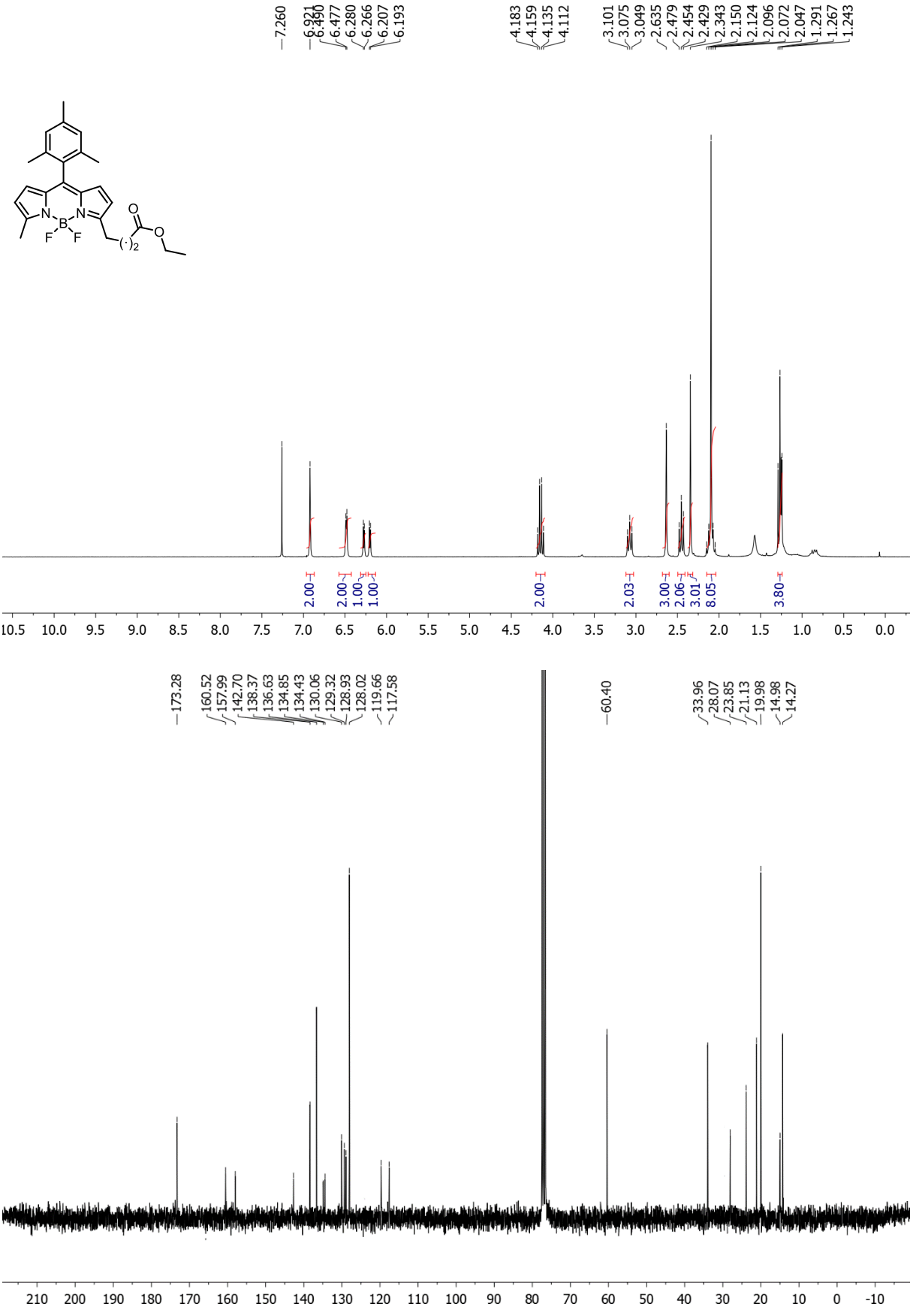

^{1}H NMR (300 MHz, $CDCl_3$) and ^{13}C NMR (75 MHz, $CDCl_3$) spectra of **8**

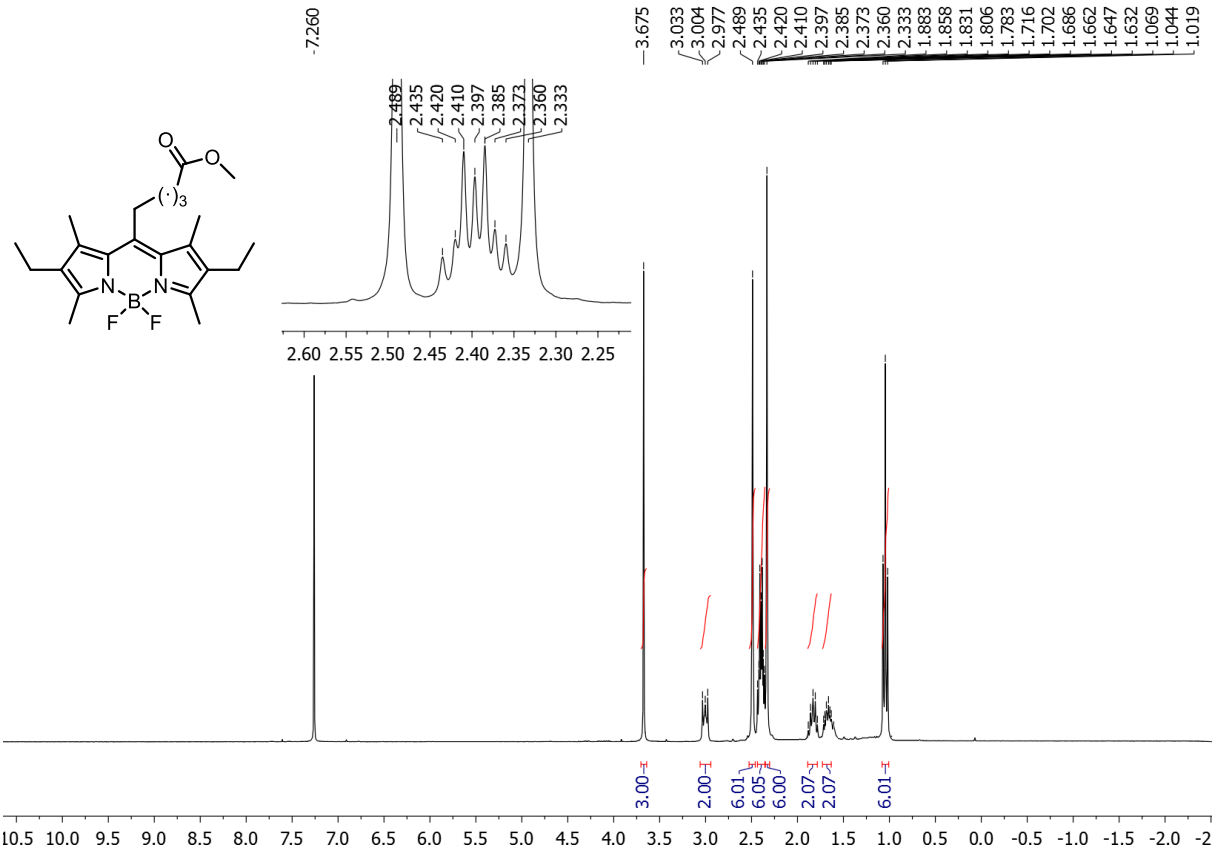

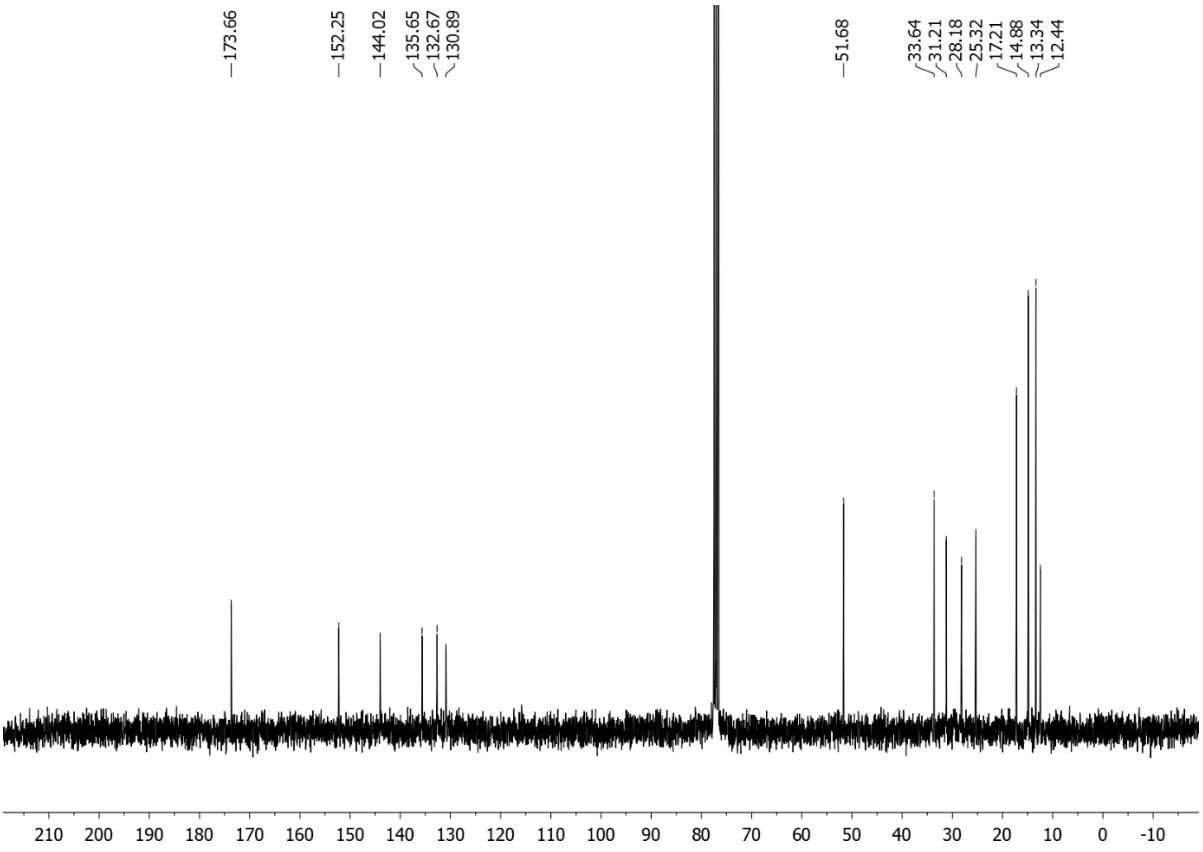

^{1}H NMR (700 MHz, $CDCl_3$) and ^{13}C NMR (176 MHz, $CDCl_3$) spectra of **9**

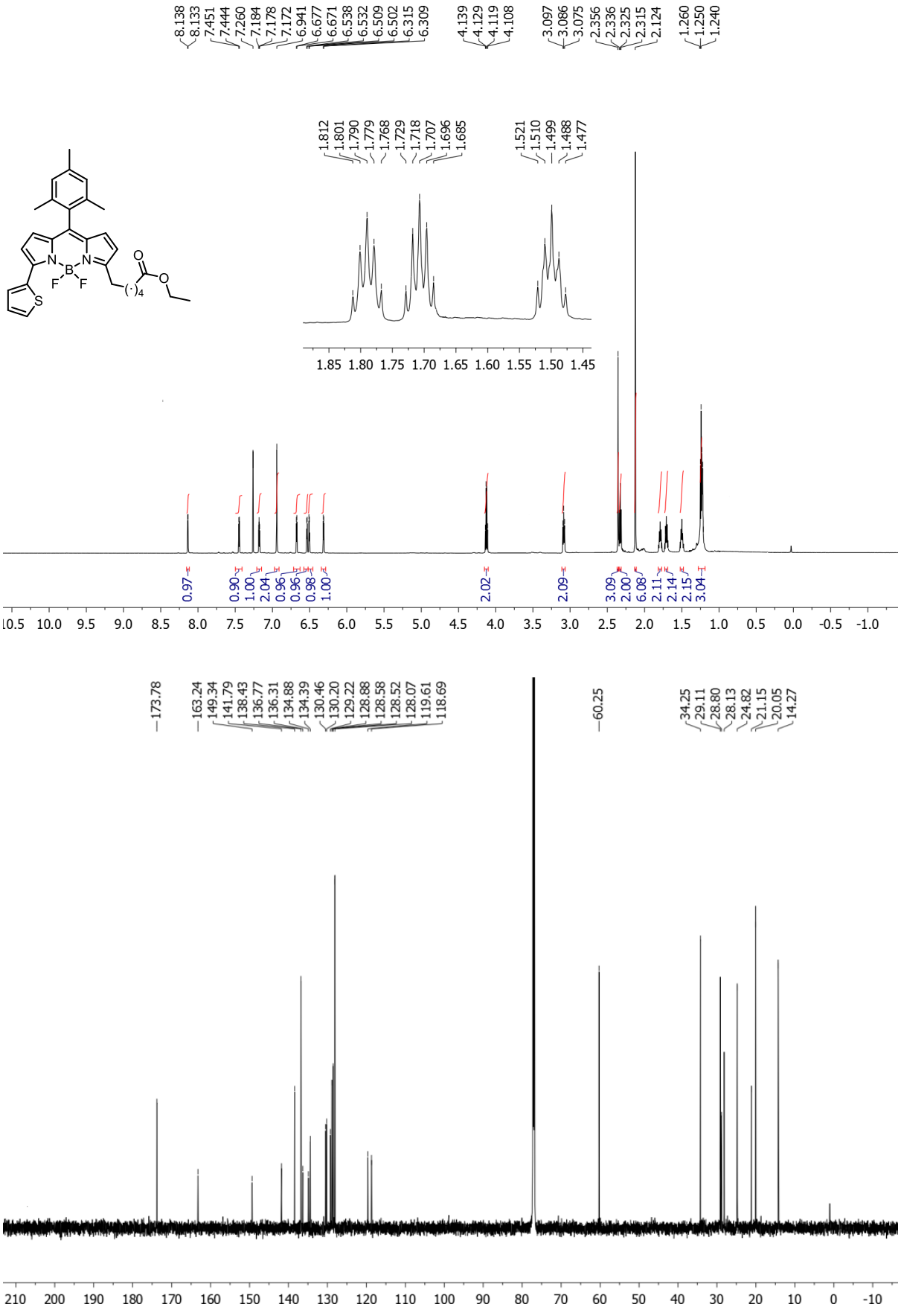

6. References

1. G. Durán-Sampedro, A. R. Agarrabeitia, L. Cerdán, M. E. Pérez-Ojeda, A. Costela, I. García-Moreno, I. Esnal, J. Bañuelos, I. López-Arbeloa and M. J. Ortiz, *Adv. Funct. Mater.,* 2013, **23**, 4195.
2. J. C. Stockert, M. I. Abasolo, A. Blázquez-Castro, R. W. Horobin, M. Revilla and D. M. Lombardo, *Biotech. Histochem*., 2010, **85**, 277.
3. J. L. Ramirez-Zacarias, F. Castro-Muñozledo and W. Kuri-Harcuch, *Histochem*., 1992, **97**, 493.
4. H. Wang and J. A. Joseph, *Free Radic. Biol. Med.,* 1999, **27**, 612.
5. J. R. Harbour and S. L. Issler, *J. Am. Chem. Soc.* 1982, **104**, 903.
6. S. Rello, J. C. Stockert, V. Moreno, A. Gamez, M. Pacheco, A. Juarranz, M. Cañete and A. Villanueva, *Apoptosis*, 2005, **10**, 201.
7. S. J. Riedl and G. S. Salvesen, *Nat. Rev. Mol. Cell. Biol.*, 2007, **8**, 405.
8. (*a*) S. Kusaka, R. Sakamoto, Y. Kitagawa, M. Okumura and H. Nishihara, *Chem. Asian J*., 2012, **7**, 907; (*b*) J. H. Kim, H. S. Kim, PCT Int Appl 2015, WO 2015064864 A1.
9. V. Leen, E. Braeken, K. Luckermans, C. Jackers, M. Van der Auweraer, N. Boens and W. Dehaen, *Chem. Commun*., 2009, 4515.
10. T. Sakida, S. Yamaguchi and H. Shinokudo, *Angew. Chem. Int. Ed.*, 2011, **50**, 2280.